JOURNAL OF CATALYSIS 147, 231–240 (1994)

Computer-Assisted Screening of Zeolite Catalysts for the Selective Isopropylation of Naphthalene

J. A. Horsley,* J. D. Fellmann,[1,*] E. G. Derouane,† and C. M. Freeman‡

*Catalytica, Inc., 430 Ferguson Drive, Mountain View, California 94043; †Laboratoire de Catalyse, Facultes Universitaires N-D de la Paix, B-5000 Namur, Belgium; and ‡BIOSYM Technologies, Inc., 9685 Scranton Road, San Diego, California 92121

Received May 25, 1993; revised January 3, 1994; accepted January 5, 1994

Molecular graphics screening of potential zeolite catalysts for the selective synthesis of 2,6-diisopropylnaphthalene indicated that mordenite was a promising candidate. Molecular mechanics calculations of the minimum energy pathway for diffusion of the diisopropylnaphthalene isomers in mordenite showed that significant energy barriers exist for the 2,7 isomer, while the diffusion of the 2,6 isomer is unimpeded. In the case of zeolite L, no significant energy barrier was found for either isomer. In an experimental study of naphthalene isopropylation in a batch autoclave reactor, mordenite produced a 2,6/2,7 ratio of 2.5, while zeolite L was essentially nonselective. The combination of molecular graphics and molecular mechanics appears to be a powerful and reliable method for the screening of zeolites for selective catalysis. © 1994 Academic Press, Inc.

INTRODUCTION

Computational modeling of zeolites and adsorbed molecules is potentially a very efficient method of screening possible catalysts for shape-selective reactions. Using molecular graphics it is possible to rapidly visualize how well the various reactant or product molecules fit in the pores of candidate zeolites (1). Quantitative molecular mechanics (2–4) or molecular dynamics (5) studies of the diffusion in the pores can provide confirmation of the molecular graphics results. In this paper we report the results of a computational study aimed at screening catalysts for the production of a commercially important intermediate, 2,6-diisopropyl naphthalene (DIPN) (see I). The predictions of the computational study are compared to the results of reactor tests of various catalysts for naphthalene isopropylation.

Linear dialkylated naphthalenes are gaining importance as intermediates in the manufacture of liquid crystal polymers and promising specialty polymers, such as poly(ethylenenaphthalate) (PEN) (6). The dialkylated species of choice is 2,6-DIPN (7). This species can be synthesized by isopropylation of naphthalene with propylene over solid acid catalysts. However, amorphous solid acid catalysts, such as silica–alumina, produce a mixture of isomers containing equal amounts of 2,6- and 2,7-DIPN (II) (8). Separation of the 2,6 and 2,7 isomers is difficult and costly. The high cost of monomers is presently inhibiting the growth of the market for specialty polymers, so there is a strong incentive to develop a process that would produce 2,6-DIPN selectively.

I

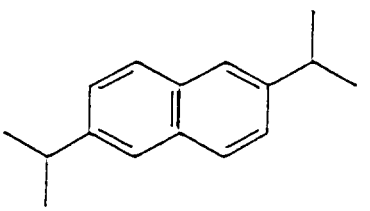

II

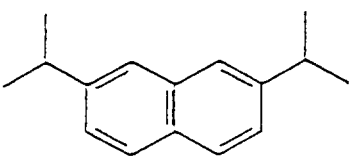

Although the average molecular dimensions of the two DIPN isomers are very similar, differences in the molecular shapes may give rise to significantly different rates of diffusion in certain zeolites. Zeolites are also solid acids, with acidity that can be varied over a wide range. Zeolites are therefore strong candidates as catalysts for the selective production of 2,6-DIPN. A number of zeolites have pore dimensions that could make them selective catalysts for 2,6-DIPN. We carried out a preliminary screening process using molecular graphics to identify the most promising zeolites for testing in a reactor. Quantitative molecular mechanics calculations of the diffusion of the DIPN isomers in selected zeolites were carried out to provide confirmation of the molecular graphics results.

[1] Present address: Salutar Inc., 428 Oakmead Parkway, Sunnyvale, CA 94086.

0021-9517/94 $6.00

METHODS

Computational

The molecular graphics screening of potential zeolite catalysts was carried out using the program Insight II (9) on Silicon Graphics Iris workstations. A space-filling model of one of the DIPN isomers was placed inside a similar model of the pore of a candidate zeolite, and its position was adjusted on the screen until the best fit between molecule and zeolite was observed.

The molecular mechanics representation of the potential energy of the sorbate in the zeolite contained terms corresponding to deformation of bond lengths and bond angles, torsions, and deviations from planarity in the case of the sorbate, while the zeolite lattice was held fixed. The potential energy also included the internal nonbonded interaction potentials for the sorbate and the nonbonded interaction potentials between the atoms of the sorbate and those of the zeolite. The potential parameters used in the calculation were taken from the consistent valence force field of Hagler *et al.* (10), and are shown in Table 1. The nonbonded interaction potentials were of the Lennard–Jones form with the addition of a term describing the electrostatic interaction,

$$E_{nb} = \sum_i \sum_{j>i} [A_{ij}/r_{ij}^{12} - B_{ij}/r_{ij}^{6} + q_i q_j / r_{ij}],$$

where q_i and q_j are partial atomic charges, and the summation extends over all pairs of atoms i, j.

The molecular mechanics calculations were carried out using the program Discover (11).

Experimental

Analytical grade naphthalene was obtained from Aldrich and was used without purification. Analytical grade propylene was obtained from Linde. Hydrogen mordenite was obtained from Tosoh, Norton, and LGP. Hydrogen L was obtained from Tosoh.

A stirred 300-cm^3 stainless steel autoclave was used in all tests. The propylene feed system consisted of a heated reservoir of propylene gas. The propylene was manually introduced (via a needle valve) into the reactor in such a way that a constant reaction pressure could be maintained throughout the experiment.

The purity of the starting materials and the composition of the reactor effluent were determined by gas chromatography on a Hewlett–Packard capillary 5880 gas chromatograph fitted with an FID.

H–mordenite catalysts supplied by the manufacturer displayed unacceptable catalyst life, presumably due to excessive coking. Improvements in catalyst life were achieved using dealuminated H–mordenite. Maximum catalyst life was achieved using a mild dealumination technique such as gentle catalyst steaming followed by a dilute acid wash and calcination. A typical dealumination was as follows: 10 g of Tosoh mordenite was loaded in a fritted quartz tube and place vertically in a tube furnace. A slow helium flow of about 200 cm^3/min was introduced into the quartz tube and the furnace was heated to 400°C. Steam-saturated helium was then introduced at a flow rate of about 1.5 liters/min. After 30 min the steam was discontinued, the helium flow was lowered to about 200 cm^3/min, and the furnace was cooled to room temperature. The solid catalyst was then transferred to a 500 ml round-bottom flask equipped with a condenser and a stir bar. After 200 ml of 0.5 *N* HCl was introduced, the resultant

TABLE 1

Parameters Used in Molecular Mechanics Calculations

Bond length parameters: $E = k_1(r - r_0)^2$

Atoms[a]		r_0 (Å)	k_1 (kcal mol^{-1} Å^{-2})
c	h	1.1050	340.6175
cp	h	1.0800	363.4164
cp	cp	1.3400	480.0000
cp	c	1.5100	283.0924

Bond angle parameters: $E = k_2(\theta - \theta_0)^2$

Atoms			θ	k_2 (kcal mol^{-1} degree^{-2})
h	c	h	106.4000	39.5000
h	c	c	110.0000	44.4000
cp	cp	h	120.0000	37.0000
cp	cp	cp	120.0000	90.0000
h	c	cp	110.0000	44.4000
c	cp	cp	120.0000	44.2000
cp	c	cp	110.5000	46.6000

Torsional parameter: $k\phi(1 + \cos(n\phi - \phi_0))$

Atoms		$k\phi$ (kcal mol^{-1})	n	ϕ_0
cp	cp	12.0000	2	180.0000

Out-of-plane parameter: $E = k\chi(1 + \cos(n\chi - \chi_0))$

Atoms[b]				$k\chi$ (kcal mol^{-1})	n	χ_0
cp	cp	cp	*	0.3700	2	180.0000

Nonbonded parameters:
$E = A_{ij}/r^{12} - B_{ij}/r^6$; $A_{ij} = (A_i A_j)^{1/2}$; $B_{ij} = (B_i B_j)^{1/2}$

Atom	A (kcal mol^{-1} Å^{12})	B (kcal mol^{-1} Å^6)
h	7108.4660	32.87076
c	1790340.7240	528.48190
o	272894.7846	498.87880
cp	2968753.3590	1325.70810
si	3149175.0000	710.00000

[a] Atom types: h, hydrogen atom; c, aliphatic carbon; o, zeolite oxygen atom; cp, aromatic carbon; si, zeolite silicon.

[b] Atom * indicates any potential parameter.

mixture was refluxed for 4 h. After cooling, the solution was filtered and washed with distilled water until the filtrate was free of chloride ion as determined by a silver nitrate test. The solid was first dried at 110°C for 2 h, followed by calcination at 500°C for at least 2 h.

A typical catalyst run used 1.0 g zeolite catalyst and 90 g naphthalene. In a standard alkylation reaction the autoclave was charged with the naphthalene feed and the zeolite catalyst. The contents were flushed with nitrogen several times and then pressurized to 12 psig with nitrogen. During slow stirring the autoclave was heated to the desired reaction temperature, at which time the stirring rate was increased to about 3200 rpm. Propylene was then added from a heated reservoir at a rate sufficient to maintain a constant pressure of 70 psig throughout the run. Samples were diluted with a hydrocarbon solvent and analyzed by GLC. Typical total reaction times were 5–7 h.

RESULTS

Molecular Graphics Screening

In the molecular graphics study large pore zeolites, such as zeolite Y, did not appear to be selective, as the fit was equally good for both isomers. Mordenite was an exception, however, because the shape of the pore matched the shape of the 2,6 isomer much better than the shape of the 2,7 isomer. For practical purposes mordenite has a nonintersecting (unidimensional) pore structure with pore dimensions of 7.0 × 6.5 Å. Figure 1 shows views of 2,6- and 2,7-DIPN in mordenite with the following van der Waals radii: Si = 0.6 Å, H = 1.10 Å, C = 1.55 Å, and O = 1.35 Å. These radii were used in the molecular graphics screening.

It is apparent from Fig. 1 that diffusion of DIPN in mordenite is governed by the cross-sectional shape of the DIPN molecule. The 2,6 isomer has a compact cross section by virtue of the fact that the three bulky components (the two isopropyl groups and the naphthalene ring) are arranged linearly. In contrast, these components are not arranged linearly in the 2,7 isomer. With both isopropyl groups placed on the same side of the naphthalene ring, the 2,7 isomer presents a less well-packed cross section in the mordenite channels as can clearly be seen in Fig. 1b.

The configurations of the DIPN isomers shown in Fig. 1 represent the molecules adsorbed on the lower part of the pore wall. For both isomers there is therefore some overlap between the DIPN molecules and the zeolite atoms in the lower region of the pore wall. However, in the case of the 2,6 isomer there is a significant amount of space between the top of the molecule and the zeolite atoms in the upper part of the pore. The 2,6 isomer can therefore desorb and move through the channel essentially unimpeded. In the case of the 2,7 isomer in Fig. 1b, in addition to the overlap in the lower part of the pore wall there is significant overlap between the upper part of the molecule and the upper part of the pore wall because of the T-shape of the molecule. Following desorption the diffusion of the 2,7 isomer will therefore be significantly impeded by steric interactions with the atoms forming the zeolite channel.

The importance of the match between the shape of the pore and the shape of the adsorbed molecule can be seen by comparing mordenite with zeolite L. The pores in zeolite L are circular, rather than elliptical, with a pore diameter of 7.1 Å. Figure 2 shows views of the 2,6- and 2,7-DIPN in zeolite L. In contrast to mordenite, there appears to be plenty of room for either 2,6- or 2,7-DIPN in the zeolite L pore. There should be no significant barriers to diffusion for either isomer in zeolite L, and hence, zeolite L would not be expected to produce 2,6-DIPN selectively.

Molecular Mechanics Calculations

The molecular graphics screening indicated that the rates of diffusion of the DIPN isomers should be significantly different in mordenite, but similar in zeolite L. However, the reliability of predictions based on visualization can only be qualitative. These predictions could in principle be tested by quantitative calculations of relative or absolute diffusion rates by means of molecular dynamics simulations of the migration of the DIPN molecules in the pores. Such calculations have been carried out for small molecules (5), but for large sorbates, such as DIPN, large scale molecular events, such as concerted translation along a channel, occur too infrequently to be observed on a typical molecular dynamics timescale (10^{-10} s). The direct dynamical simulation of the diffusion of large molecules in zeolites remains a challenging problem.

In the case of zeolites with unidimensional pore systems, the general diffusion pathway for large molecules can be defined without recourse to large scale, costly molecular dynamics calculations. The variation of the guest/host interaction energy along this pathway should provide information on the relative rates of diffusion of different guest molecules. The energy profile along the diffusion pathway can be obtained by means of molecular mechanics calculations based on empirical parameters (2–4).

We have used molecular mechanics calculations to obtain the minimum energy profiles for the diffusion of 2,6- and 2,7-DIPN in mordenite and zeolite L. The diffusion path was defined by a pair of points on the channel axis at opposite ends of the section of channel under investigation. For each step of the calculation the sorbate molecule was constrained to lie at a fixed distance from these ex-

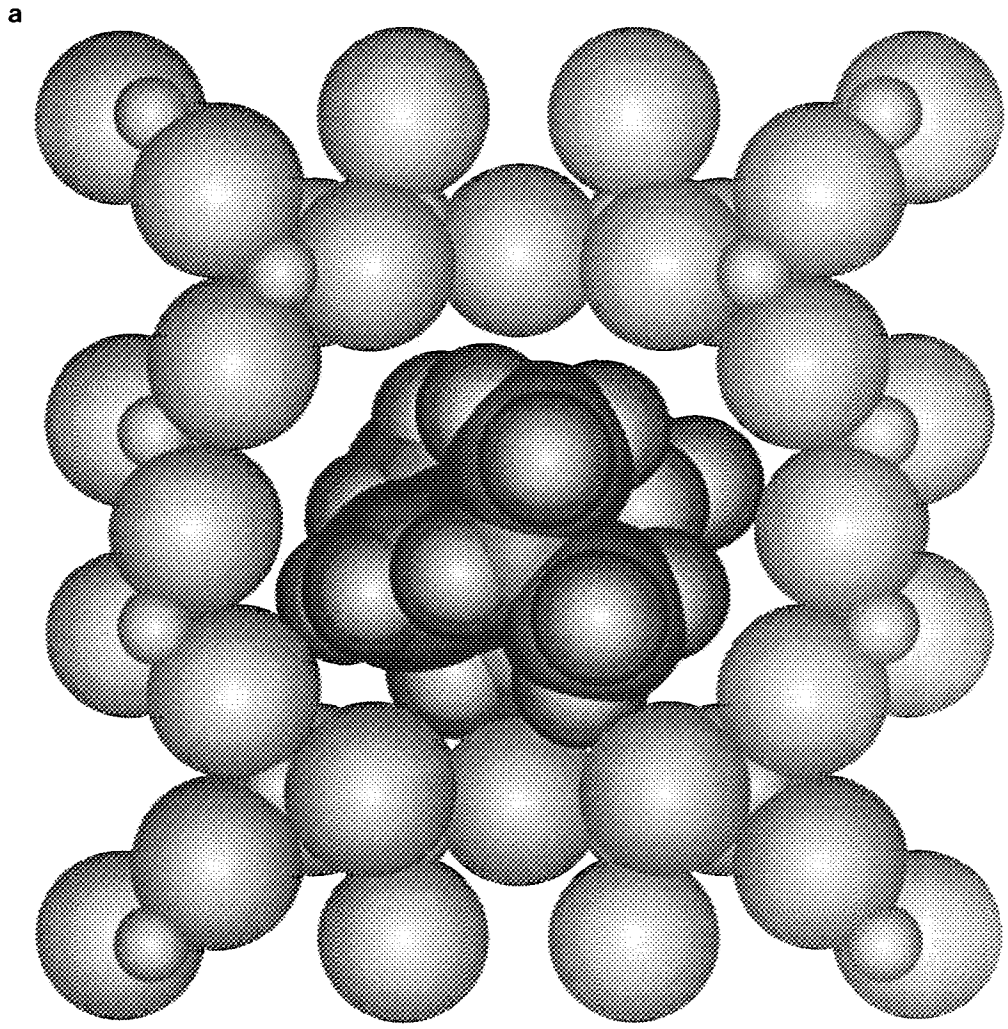

FIG. 1. Space-filling models of (a) 2,6-DIPN and (b) 2,7-DIPN in mordenite.

treme points by a strong harmonic potential. The molecule was shifted along the channel axis in the direction of diffusion in steps of 0.2 Å. The total energy of the sorbate, including the interaction with the zeolite, was minimized at each step. The zeolite lattice was held fixed at the crystallographically determined geometry (12, 13) during the minimization, while the sorbate was allowed complete freedom to optimize the interaction with the host, subject to the above distance constraints. The connected set of energy minimizations provides a minimum energy profile for diffusion of the sorbate along the zeolite channel (2–4).

The above approach does not take into account fluctuations in the size of the zeolite pore during the lattice vibrations. Deem *et al.* (14) recently reported simulations of the framework dynamics for a number of zeolites, including zeolite L. For zeolite L the simulations provided a clear demonstration of the breathing motion of the pore windows. At 550 K the maximum fluctuation in the zeolite L pore diameter was 0.3 Å, so the pore size can expand from 7.1 to 7.4 Å during the breathing motion. A similar fluctuation is expected for the mordenite pores. Thus, during the translational motion at any given instant the pore size may be significantly smaller or larger than the crystallographically determined value. However, these fluctuations take place on the timescale of a lattice vibration, approximately 10^{-13} s. Any translational motion of a large molecule along the pore will take place on a timescale many orders of magnitude longer. The crystallographically determined pore size therefore represents an average configuration during the translational motion. In the case of two isomers the minimum energy profiles calculated for this average configuration should give a good indication of the relative rates of diffusion through the pore. If the minimum energy profile shows a significantly higher energy barrier for one isomer, then the diffusion of that isomer will on average be much slower than that

b

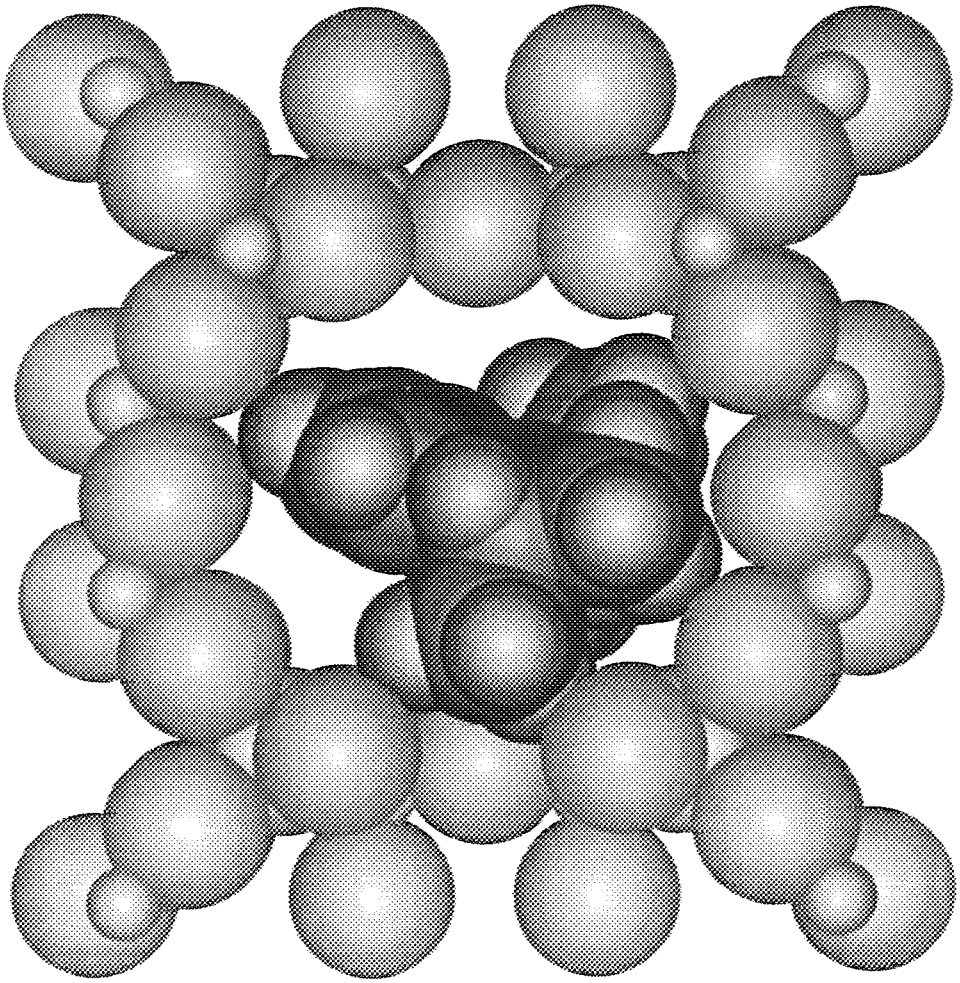

FIG. 1—*Continued*

of the other isomer. If, however, the energy barriers for the two isomers are comparable, then the diffusion rates should be approximately the same.

The interaction with the large DIPN molecules could also induce local relaxation in the zeolite framework. This relaxation would reduce the repulsive interaction between the molecule and the framework and hence would be expected to reduce somewhat the difference in the energy barriers for the two isomers. The limited flexibility of the zeolite framework will restrict the magnitude of this effect, however, and the rigid framework approximation should provide reasonably accurate diffusional barriers for the two isomers.

Figure 3 shows the calculated minimum energy profiles for the diffusion of 2,6- and 2,7-DIPN in mordenite. It is evident that the diffusion of 2,6-DIPN, with a calculated energy barrier of 4 kcal/mol, is significantly less hindered than the diffusion of 2,7-DIPN, with a calculated energy barrier of 18 kcal/mol. Figure 4 shows the position of the 2,7-DIPN in the mordenite pore at the peak of the energy barrier. It can be seen that the highest energy position corresponds to a configuration in which the isopropyl groups are both passing through pore windows. Based on the molecular graphics representation shown in Fig. 1b, this is indeed the configuration for which the steric repulsion would be expected to be at a maximum. The calculations of the minimum energy profile therefore support the prediction based on molecular graphics that mordenite should be a shape-selective catalyst for the production of 2,6-DIPN.

Minimum energy profiles were also calculated for 2,6- and 2,7-DIPN in zeolite L. However, the calculation of accurate energy profiles for the isomers in zeolite L proved to be far from straightforward. The difficulties encountered in these calculations are instructive, as they illustrate the pitfalls in calculations of the minimum energy

a

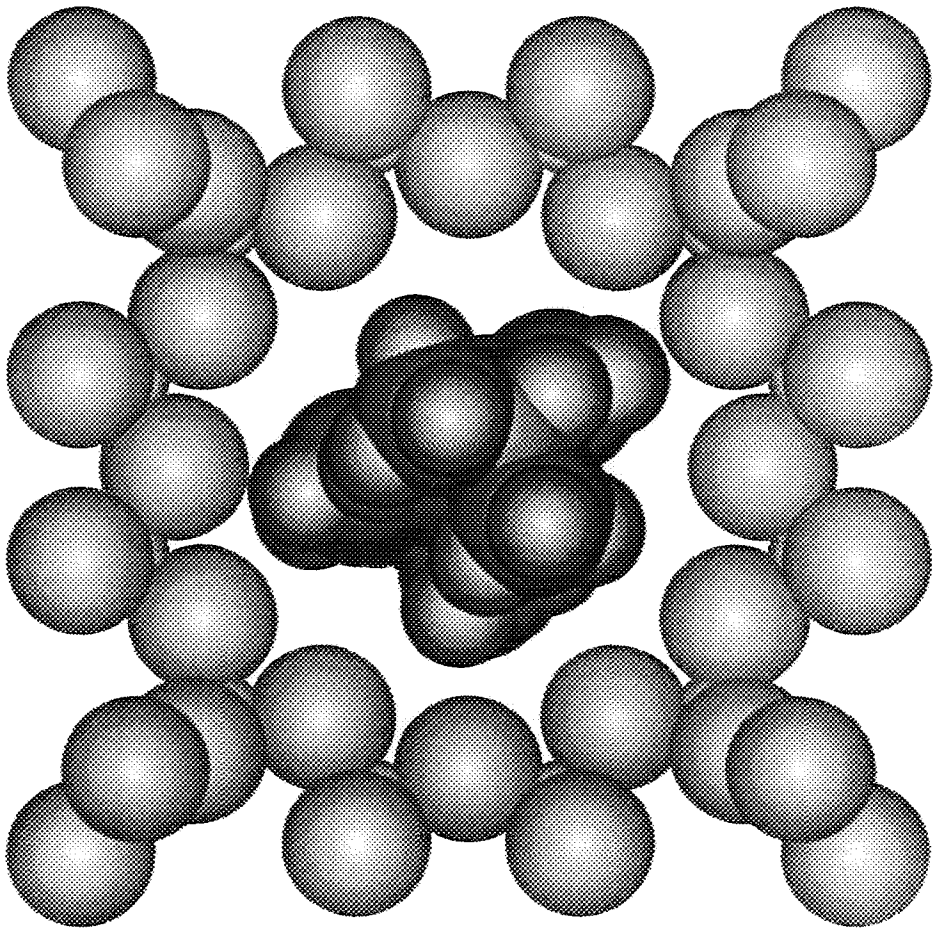

FIG. 2. Space-filling models of (a) 2,6-DIPN and (b) 2,7-DIPN in zeolite L.

pathway for diffusion in zeolites. We will therefore report the results for zeolite L in some detail.

Molecular mechanics calculations of the minimum energy profiles for 2,6- and 2,7-DIPN in zeolite L were initially performed in the same way as those for mordenite. In the case of zeolite L, however, for both isomers a series of very sharp peaks was obtained at regular intervals in a rather flat energy profile. The sharp spikes in the energy profile were most unexpected, as the molecular graphics study indicated that there should be no strong steric interaction between the two isomers and the zeolite L pore (see Fig. 2). However, a more detailed examination of the configuration of the sorbate in the region of the peaks revealed the cause of the problem.

In the regions of the pore between the windows there is sufficient room for the sorbate to adopt a tilted configuration, with the isopropyl groups nesting in the pore walls. This configuration maximizes the sorption between the sorbate and the zeolite and thus is the preferred configuration in this region of the pore. The tilted configuration for the 2,7-DIPN isomer is shown in Fig. 5. However, in order to pass through the windows the sorbate must adopt a configuration in which the naphthalene ring is parallel to the pore axis (Fig. 6). The rapid change in the preferred configuration leads to difficulties in the energy minimization, as the sorbate in the tilted configuration must pass over an energy barrier to find the new preferred configuration. The sorbate is initially trapped in a local energy minimum at the point at which the switch should occur. In the local energy minimum the molecule retains the tilted configuration. As the molecule is advanced in the direction of diffusion, the energy of this local minimum rises very sharply because the leading isopropyl group is pushed up against the pore wall if the molecule retains the tilted configuration. After advancing only a very short distance, however, the sorbate does succeed in finding the correct, nontilted configuration, and the energy immediately drops to a much lower value.

We found that using a simple Monte Carlo procedure, it was possible to insure that sudden changes in the location of the energy minimum did not trap the sorbate in a local minimum on the diffusion pathway. The Monte Carlo

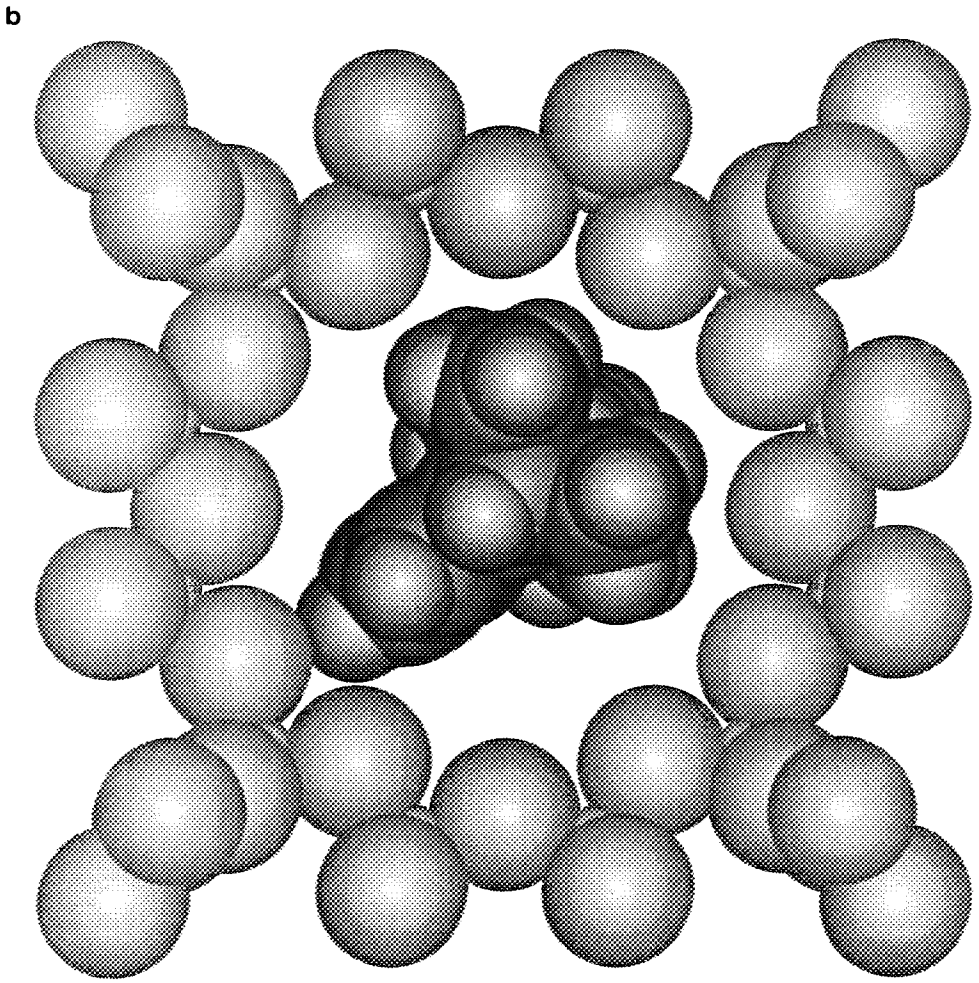

FIG. 2—*Continued*

procedure was carried out before each energy minimization. The orientation of the molecule was changed by a random perturbation and the change was accepted if it resulted in a lowering of the energy. This was repeated for 50 trials, and the configuration of lowest energy was taken as the starting point for the energy minimization.

The energy profiles for 2,6- and 2,7-DIPN in zeolite L calculated with the combined Monte Carlo and energy minimization technique are shown in Fig. 7. There is no significant energy barrier for either isomer. The calculations again confirm the molecular graphics prediction: zeolite L is not a shape-selective catalyst for production of 2,6-DIPN.

Molecular mechanics calculations of the minimum energy profile for diffusion appear to be a relatively simple and reliable way to provide quantitative support for the

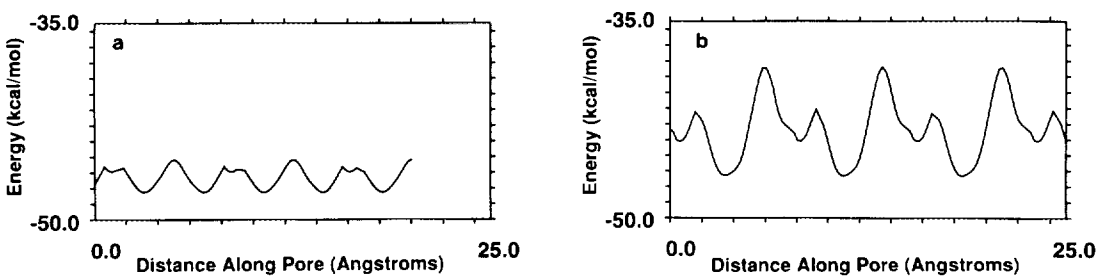

FIG. 3. Minimum energy profiles for diffusion of (a) 2,6-DIPN and (b) 2,7-DIPN in mordenite. The zero of energy corresponds to the empty zeolite plus the sorbate in the ideal gas phase.

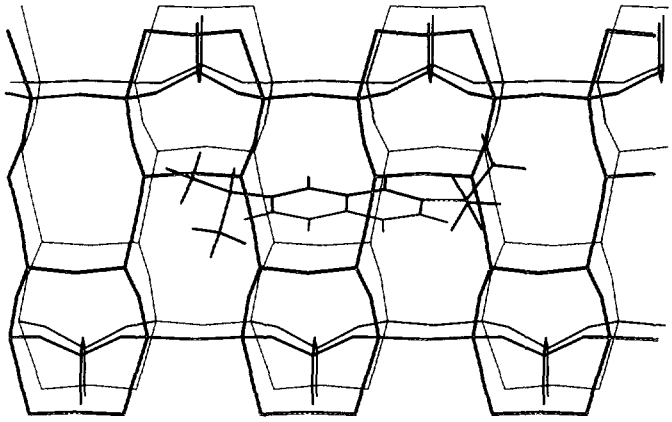

FIG. 4. Position of 2,7-DIPN in mordenite at peak of energy barrier.

results of molecular graphics screening. However, the energy profile should be checked for any sudden changes in configuration, which may result in spurious peaks. In this case, a simple Monte Carlo procedure appears adequate to correct the errors.

Confinement Effects in the Selective Production of 2,6-DIPN

The excellent fit and low diffusional barrier for 2,6-DIPN in mordenite suggest that confinement effects are important in the selective production of this isomer. Confinement catalysis in molecular sieves is based on the principles of molecular recognition and supramolecular catalysis (15, 16). Derouane (16) has stressed that the basis of confinement catalysis is entirely different from the basis of the familiar molecular shape-selective catalysis. In confinement catalysis attractive van der Waals interactions are dominant. These interactions act positively. For example, they can preorganize a substrate in a favorable configuration prior to reaction (rather like an enzyme), or they can favor molecular diffusion in the channels. In contrast, repulsive interactions that operate by exclusion are dominant in molecular shape-selective catalysis.

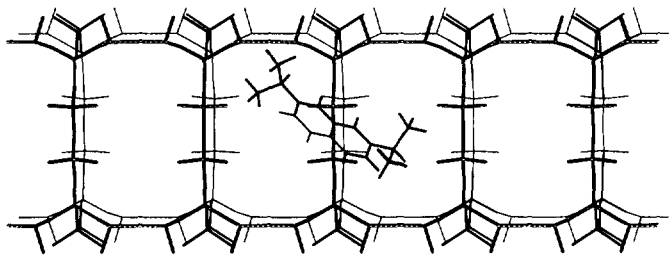

FIG. 5. Tilted configuration of 2,7-DIPN in zeolite L between the pore windows.

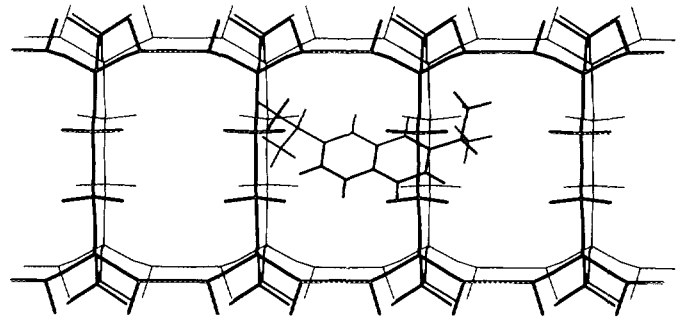

FIG. 6. Parallel configuration of 2,7-DIPN in zeolite L as it passes through the pore windows.

Molecules adsorbed on the pores of molecular sieves often show important confinement effects because the curvature of the surface of the pore wall amplifies van der Waals interactions (15). In particular, in the case in which there is an excellent fit between the molecular dimensions and the channel dimensions, the molecules acquire supermobility, i.e., they behave as "floating molecules" because the strong van der Waals interaction is approximately equal in all directions. 2,6-DIPN in mordenite appears to be an example of such a floating molecule. For the 2,6 isomer the attractive forces are dominant and the repulsive forces play a very small role, so the diffusion of this isomer can be said to be determined by confinement effects. In contrast, the 2,7 isomer will not be supermobile because for certain sections of the pore, the fit is not as good as the fit for the 2,6 isomer, leading to significant potential barriers. There will therefore be a large difference in the diffusion rates of the two isomers.

The difference in diffusion rates between the DIPN isomers in mordenite can give rise to selective production of 2,6-DIPN by a mechanism similar to that proposed by Olson and Haag (17) for the selective production of *p*-xylene by the alkylation of toluene in ZSM-5. The DIPN isomers in mordenite will undergo rapid acid-catalyzed isomerization and equilibration, similar to the equilibration among the xylenes in ZSM-5. The more rapidly diffusing 2,6 isomer will be removed from the zeolite pores at a faster rate than the slower 2,7 isomer, which will continually shift the equilibrium between the isomers toward production of the 2,6 isomer.

Factors other than the difference in the diffusion rates may also contribute to the selectivity, however. There may be a contribution to the selectivity from the isopropylation reaction itself, through transition state selectivity. The transition state for formation of 2,7-DIPN from isopropylnaphthalene can reasonably be assumed to have a somewhat "bent" configuration, like 2,7-DIPN itself. The transition state for the 2,6-DIPN would be more "linear." Based on the minimum energy profiles for the DIPN iso-

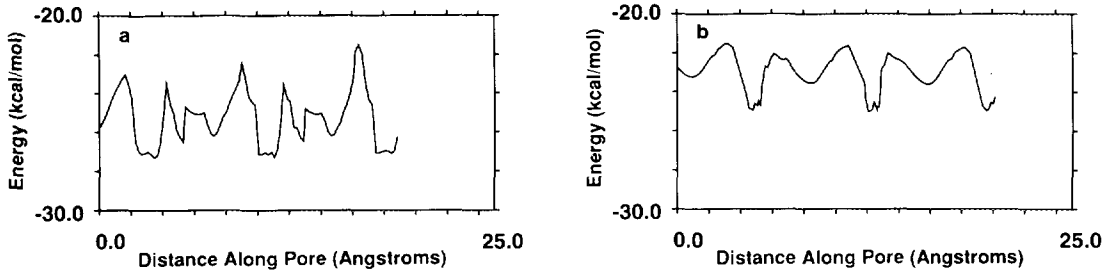

FIG. 7. Minimum energy profiles for the diffusion of (a) 2,6-DIPN and (b) 2,7-DIPN in zeolite L.

mers in mordenite (Fig. 3), the transition state for the formation of 2,7-DIPN would have on average a higher energy than the transition state for formation of 2,6-DIPN, resulting in a higher activation energy for production of the 2,7 isomer. However, any selectivity in the initial production of the isomers would probably be eliminated by the subsequent rapid acid-catalyzed isomerization and equilibration.

It is also possible that the acid-catalyzed isomerization reaction could contribute to the selectivity. As the 2,7 isomer has on the average a higher energy than the 2,6 isomer in the pore (Fig. 3), the equilibrium will tend to favor the 2,6 isomer, whereas gas-phase equilibration would produce a 50 : 50 mixture.

Experimental Results and Discussion

The results of the reactor tests for mordenite, zeolite L, and amorphous silica–alumina are summarized in Table 2. The amorphous catalyst produces equal amounts of the two isomers. In contrast, mordenite shows a high selectivity for the formation of the 2,6 isomer, consistent with the results of the molecular graphics and molecular mechanics study. A similar high selectivity for formation of 2,6-DIPN in mordenite was observed by Katayama *et al.* (18) but not by Moreau *et al.* (19).

Zeolite L shows a small selectivity for production of the 2,7 isomer. The origin of this selectivity is not clear. The molecular mechanics calculations indicate that the diffusion of the DIPN isomers in zeolite L is complex, involving a sudden change of the molecular orientation in the pore. The observed selectivity could be due to a slightly different response of the two isomers to the sudden change in configuration. The energy barriers in the calculated minimum energy profiles are indeed slightly higher for 2,6-DIPN (4.0–6.0 kcal/mol) than for 2,7-DIPN (3.5–4.0 kcal/mol). This difference probably reflects a somewhat better fit for the 2,7 isomer in the region between the windows where the isopropyl group is nested in the pore wall (Fig. 5). However, it is not clear that such a small difference in energy barriers could lead to any significant difference in diffusion rates at the reaction temperature. More detailed simulations of the diffusion of the DIPN isomers in zeolite L, including molecular dynamics studies, are needed in order to shed more light on the observed selectivity in this zeolite.

Overall, however, the results of the catalyst tests bear out the predictions of the molecular graphics and molecular mechanics calculations. Although these calculations are not able to predict unambiguously the observed selectivity for zeolite L, this selectivity is very small and favors the undesired isomer.

The good agreement between experiment and theory confirms the reliability of molecular modeling methods in

TABLE 2

Selectivity of Catalysts in the Isopropylation of Naphthalene with Propylene[a]

Catalyst	Naphthalene conversion (%)	Isopropylnaphthalene selectivities (mol%)			Ratio 2,6-/2,7-DIPN	2,6-DIPN in total DIPN (%)
		mono	di	poly		
Mordenite[b]	54.5	73.9	25.7	0.46	2.51	60.4
Zeolite L	69.0	77.8	20.6	1.60	0.82	21.8
SiO_2–Al_2O_3[c]	23.5	91.9	8.1	0.0	1.00	36.8
	94.2	31.1	51.5	17.4	1.03	38.5

[a] Batch autoclave reactor at 275°C.
[b] Dealuminated according to the procedure described in experimental section.
[c] Source: W. R. Grace; SiO_2/Al_2O_3 = 2.98.

the screening of zeolites for shape-selective reactions. Molecular graphics can be used to narrow down the selection to a small number of promising candidates, and the most promising of these candidates can be identified on the basis of molecular mechanics calculations of the minimum energy pathways for diffusion of the target molecules through the zeolite pores. As the computational techniques are much less time-consuming than testing a range of zeolites in a reactor, it is expected that these techniques will increasingly replace empirical screening in the selection of zeolite catalysts.

CONCLUSIONS

Molecular graphics and molecular mechanics studies have provided a reliable basis for choosing a shape-selective catalyst for the isopropylation of naphthalene. Mordenite is a highly selective catalyst for the production of 2,6-DIPN, and zeolite L is almost completely nonselective, as predicted. Zeolite L shows a very small selectivity toward 2,7-DIPN that may be connected to a rapid change in minimum energy configuration as the molecules diffuse along the pore.

Calculation of the minimum energy profile for diffusion along the zeolite pore is a useful means of confirming the results of a visual inspection. However, rapid changes in the minimum energy configuration may give rise to spurious peaks in the energy profile. These peaks can be removed using a simple Monte Carlo procedure.

REFERENCES

1. Freeman, C. M., Levine, S. M., Newsam, J. M., Sauer, J., Tomlinson, S. M., Brickmann, J., and Bell, R. G., *in* "Modelling of Structure and Reactivity in Zeolites" (C. R. A. Catlow, Ed.), p. 133. Academic Press, London, 1992.
2. Pickett, S. D., Nowak, A. K., Thomas, J. M., and Cheetham, A. K., *Zeolites* **9,** 123 (1989).
3. Schroder, K-P., and Sauer, J., *Z. Phys. Chem. (Leipzig)* **271,** 289 (1990).
4. Nakazaki, Y., Goto, N., and Inui, T., *J. Catal.* **136,** 141 (1992).
5. Demontis, P., and Suffritti, G. B., *in* "Modelling of Structure and Reactivity in Zeolites" (C. R. A. Catlow, Ed.), p. 79. Academic Press, London, 1992.
6. Trotter, J. R., and Sublett, B. J., U.S. Patent 5,013,820 (1991).
7. Sanchez, P. A., Young, D. A., Kuhlmann, G. E., Partenheimer, W., Schammel, W. P., U.S. Patent 4,950,786 (1990).
8. Newman, S. F., Fellmann, J. D., and Kilner, P. H., U.S. Patent 5,003,120 (1991).
9. Insight II, BIOSYM Technologies, Inc., San Diego, CA.
10. Hagler, A. T., Lifson, S., and Dauber, P., *J. Am. Chem. Soc.* **101,** 5122 (1979).
11. Discover, BIOSYM Technologies, Inc., San Diego, CA.
12. Alberti, A., Davoli, P., and Vezzalini, G., *Z. Kristallogr.* **175,** 249 (1986).
13. Newsam, J. M., *J. Phys. Chem.* **93,** 7689 (1989).
14. Deem, M. W., Newsam, J. M., and Creighton, J. A., *J. Am. Chem. Soc.* **114,** 7198 (1992).
15. Derouane, E. G., Andre, J-M., and Lucas, A. A., *J. Catal.* **110,** 58 (1988).
16. Derouane, E. G., *in* "Guidelines for Mastering the Properties of Molecular Sieves" (D. Barthomeuf, E. G. Derouane, and W. Holderich, Eds.), NATO ASI Series B: Physics, Vol. 221, p. 225. Plenum Press, New York, 1990.
17. Olson, D. H., and Haag, W. O., *in* "Catalytic Materials: Relationship between Structure and Reactivity" (T. E. Whyte, R. A. Dalla Betta, E. G. Derouane, and R. T. K. Baker, Eds.), ACS Symposium Series, Vol. 248, p. 275. Amer. Chem. Soc., Washington, DC, 1984.
18. Katayama, A., Taba, M., Takeuchi, G., Mizukami, F., Niwa, S., and Mitamura, S., *J. Chem. Soc., Chem. Commun.*, 39 (1991).
19. Moreau, P., Finiels, A., Geneste, P., and Solofo, J., *J. Catal.* **136,** 487 (1992).